Research Square

Preprints are preliminary reports that have not undergone peer review.
They should not be considered conclusive, used to inform clinical practice,
or referenced by the media as validated information.

Benchmark Validation of the Direct Mathematical Method for HPGe Detector Efficiency Calibration Against Experimental Data, EFFTRAN, and Geant4-Based RayXpert Simulations

Mahmoud Ibrahim Abbas

mabbas@physicist.net

Alexandria University

Research Article

Keywords: HPGe detector, Full-energy peak efficiency, Direct Mathematical Method, EFFTRAN, RayXpert, Geant4, Efficiency calibration, Gamma-ray spectrometry

Posted Date: November 26th, 2026

DOI: https://doi.org/10.21203/rs.3.rs-11799622/v1

License: This work is licensed under a Creative Commons Attribution 4.0 International License. Read Full License

Additional Declarations: No competing interests reported.

Abstract

Accurate full-energy peak efficiency (FEPE) calibration of high-purity germanium (HPGe) detectors is essential for quantitative gamma-ray spectrometry and numerous applications in nuclear science and technology. Although Monte Carlo radiation-transport simulations and efficiency-transfer techniques are widely employed for detector efficiency determination, their implementation often requires detailed detector characterization and considerable computational effort. In the present study, the Direct Mathematical Method (DMM) was evaluated as an analytical alternative through comparison with experimental measurements, EFFTRAN calculations, and Geant4-based RayXpert simulations reported for a 78.5% relative-efficiency n-type coaxial HPGe detector.

The detector-response parameter required by the DMM, namely the effective photopeak attenuation coefficient, was derived from the experimental efficiency data and subsequently used to predict FEPE values over a wide gamma-ray energy range. Calculated efficiencies were compared with experimental, EFFTRAN, and RayXpert results using relative-deviation analysis together with statistical performance indicators, including the coefficient of determination (R^2), root-mean-square error (RMSE), and mean absolute percentage error (MAPE).

The DMM accurately reproduced the experimental efficiency curve across the investigated energy range, yielding absolute relative deviations ranging from 0.09% to 0.92%, with a mean absolute deviation of only 0.38%. These results demonstrate substantially better agreement with the experimental data than both RayXpert and EFFTRAN. The findings indicate that the DMM provides a reliable and computationally efficient framework for HPGe detector efficiency calibration and detector-response characterization, demonstrating that the DMM constitutes an accurate and computationally efficient alternative to both Monte Carlo-based and efficiency-transfer methodologies for HPGe detector efficiency calibration.

1. Introduction

High-purity germanium (HPGe) detectors are widely recognized as the benchmark instrumentation for high-resolution gamma-ray spectrometry because of their excellent energy resolution and superior radionuclide identification capability. As a result, HPGe detectors play a central role in environmental radioactivity monitoring, neutron activation analysis, nuclear safeguards, radioactive waste characterization, geological investigations, and reactor-related applications. Accurate determination of full-energy peak efficiency (FEPE) is fundamental to quantitative gamma-ray spectrometry because the uncertainty associated with detector efficiency directly affects radionuclide activity measurements and subsequent analytical conclusions [1–4].

Experimental efficiency calibration using certified radioactive sources remains the most reliable approach for FEPE determination. Nevertheless, experimental calibration procedures are often time-consuming, expensive, and restricted by the availability of suitable reference materials covering the required energy range and source-detector geometries. These limitations have motivated the development of several computational methodologies for detector efficiency estimation.

Monte Carlo radiation-transport codes, including Geant4, MCNP, and PENELOPE, have become standard tools for detector efficiency simulation because they model photon interactions in detector materials with high accuracy [5–9]. Despite their proven reliability, these methods generally require detailed knowledge of detector construction parameters and may involve substantial computational effort, especially when realistic source geometries and heterogeneous matrices are involved.

Efficiency-transfer techniques provide an alternative strategy by deriving efficiencies for unknown geometries from a previously established reference calibration. Among these methodologies, EFFTRAN has achieved widespread acceptance owing to its balance between computational efficiency and predictive accuracy for practical gamma-spectrometry applications [10–12].

Analytical methods offer another attractive approach for detector efficiency determination. The Direct Mathematical Method (DMM), originally developed by Abbas, establishes an explicit analytical relationship between detector efficiency and an effective photopeak attenuation coefficient while incorporating detector geometry through compact mathematical expressions [13–19]. Previous investigations have demonstrated that the DMM can provide accurate efficiency predictions with significantly lower computational demands than simulation-based approaches. Nevertheless, comprehensive validation of the DMM against state-of-the-art Monte Carlo and efficiency-transfer methodologies using common experimental benchmark datasets remains limited. Recently, Demirel, et al. [1] reported a detailed efficiency-calibration study for a 78.5% relative-efficiency n-type coaxial HPGe detector using experimental measurements, EFFTRAN calculations, and Geant4-based RayXpert simulations. The study employed well-characterized detector geometry and well-defined cylindrical calibration sources, providing a suitable benchmark dataset for validation of alternative efficiency-calculation methods.

The objective of the present work is to assess the predictive capability of the Direct Mathematical Method by comparing its calculated efficiencies with the corresponding experimental, EFFTRAN, and RayXpert results reported by Demirel et al. Effective photopeak attenuation coefficients were first derived from experimental FEPE data and subsequently employed to calculate efficiencies across the investigated energy range. The performance of the DMM was evaluated using relative-deviation analysis and statistical indicators, including R^2, RMSE, and MAPE. Special emphasis was placed on the low-energy region, where attenuation, detector geometry, and source self-absorption exert the strongest influence on detector response.

2. Theoretical Formulation

The absolute full-energy peak efficiency (FEPE), ϵ , for an arbitrarily positioned isotropically emitting point source located at any position relative to the detector can be expressed as

$$\epsilon = \frac{1}{4\pi}\int_{\Omega} F_{att}(E).\left[1-\exp(-\mu\, d)\right] d\Omega \qquad (1)$$

where θ and ϕ denote the polar and azimuthal angles, respectively, μ is the linear photopeak attenuation coefficient [24] of the HPGe detector crystal, and d represents the effective photon path length traversed within the active detector volume. The term Ω corresponds to the solid angle subtended by the detector at the source position. The attenuation factor, $F_{att}(E)$, accounts for photon absorption in the source encapsulation, detector endcap, dead layers, and other intervening materials, and is given by

$$F_{att}(E) = \exp\left(-\sum_{i}\mu_{i}\delta_{i}\right) \qquad (2)$$

where μ_{i} is the linear attenuation coefficient [24] of the i^{th}absorbing medium at photon energy E_{γ} , and δ_{i} represents the corresponding photon path length through that material. The determination of the photon path length d constitutes the fundamental step in evaluating detector efficiency. For each emitted photon that intercepts the detector active volume, the interaction probability depends on the distance traveled inside the Germanium crystal, which varies according to the source position and photon trajectory.

2.1 Absolute Efficiency of a Non-Axial Point Source

Consider an isotropically emitting point source $P(\rho, h)$located at a radial distance ρ from the detector symmetry axis and an axial distance $h$from the detector entrance surface. Unlike the axial configuration, the off-axis source position lacks rotational symmetry; therefore, both the polar angle θ and the azimuthal angle ϕ must be considered in the efficiency calculation.

Photons entering the active germanium crystal through the detector front surface may leave the crystal through either the detector base or the cylindrical lateral surface. A photon may leave the crystal through the detector base, corresponding to an interaction path length

$$d_1 = \frac{L}{\cos\theta}, \qquad (3)$$

or through the cylindrical lateral surface, for which the path length is expressed as

$$d_2 = \frac{M(\phi)}{\sin\theta} - \frac{h}{\cos\theta}, \qquad (4)$$

where $L$and Rdenote the active crystal length and radius, respectively. The quantity $M(\phi)$represents the distance between the projection of the point source onto the detector front face and an arbitrary point on the detector circumference. Owing to the off-axis source position, this distance depends on the azimuthal angle and is given by

$$M(\phi) = \rho\cos\phi + \sqrt{R^2 - \rho^2\sin^2\phi}\,. \qquad (5)$$

The absolute full-energy peak efficiency (FEPE) for photons of energy E_{γ} emitted from the non-axial point source can therefore be written as

$$\epsilon(E,\rho,h) = \frac{1}{4\pi}\int_{0}^{2\pi} F_{\text{att}}(E)\left[\int_{0}^{\theta_1}\left(1-e^{-\mu\, d_1}\right)\sin\theta\,\hspace{0.17em}d\theta + \int_{\theta_1}^{\theta_2}\left(1-e^{-\mu\, d_2}\right)\sin\theta\,\hspace{0.17em}d\theta\right] d\phi\,, \quad (6)$$

where

$$\theta_1 = \tan^{-1}\hspace{0.17em}\left(\frac{M(\phi)}{L+h}\right), \qquad (7)$$

and

$$\theta_2 = \tan^{-1}\hspace{0.17em}\left(\frac{M(\phi)}{h}\right). \qquad (8)$$

The attenuation factor $F_{\text{att}}(E)$accounts for photon attenuation in all materials located between the source and the active germanium crystal, including source encapsulation, detector housing, entrance window, dead layers, and air gaps. The formulation described above provides a rigorous analytical representation of the detector response for arbitrarily positioned point sources while avoiding the computational complexity commonly associated with Monte Carlo radiation-transport simulations.

2.2 Absolute Efficiency of a Concentric Coaxial Circular Disk Source

Consider a circular disk source of radius Spositioned coaxially with the detector symmetry axis and parallel to the detector entrance surface. The source radius is assumed to satisfy

$$S \leq R,$$

where $R$is the active radius of the HPGe detector. Since the disk source may be regarded as a continuous distribution of infinitesimal point sources over its surface, the detector efficiency can be obtained by integrating the point-source efficiency across the entire source area.

The absolute FEPE of the disk source is therefore given by

$$\epsilon_{\text{disk}}(E) = \frac{2}{S^2}\int_0^S \rho \,\epsilon(E, \rho, h)\, d\rho, \qquad (9)$$

where $\epsilon(E, \rho, h)$is the point-source efficiency defined by Eq. (6). The factor $2\rho/S^2$represents the normalized radial distribution over the circular source area. This expression establishes the basis for extending the analytical formulation to volumetric cylindrical sources employed in practical calibration measurements.

2.3 Absolute Efficiency of a Concentric Coaxial Cylindrical Source

Cylindrical volume sources are frequently encountered in environmental radioactivity measurements and detector-calibration applications. Consider a cylindrical source of radius $S$and height H, positioned concentrically with the detector axis at a distance $h_0$from the detector entrance surface, as illustrated schematically in Fig. 1.

The cylindrical source may be represented as a stack of differential disk sources distributed along the source height. Consequently, the overall detector efficiency can be determined by integrating the disk-source efficiency over the source volume while accounting for source self-attenuation effects. The absolute FEPE for the cylindrical source is therefore expressed as

$$\epsilon_{cyl}(E) = \frac{1}{H}\int_{h_0}^{h_0+H} F_{\text{self}}(E)\,\epsilon_{\text{disk}}(E)\, dh, \qquad (10)$$

where $F_{\text{self}}(E)$ denotes the self-absorption correction factor within the sample matrix and ϵ_{disk} is the disk-source efficiency obtained from Eq. (9).

This formulation incorporates both geometrical and attenuation effects within a compact analytical framework and enables the calculation of detector efficiencies for realistic volumetric calibration sources without requiring detailed Monte Carlo simulations.

2.4 True Coincidence Summing Correction for a Concentric Coaxial Cylindrical Source

True coincidence summing (TCS) occurs when two or more radiations emitted during the same nuclear decay are detected simultaneously within the resolving time of the spectrometry system. In HPGe gamma-ray spectrometry, this phenomenon may produce summing-out losses from individual full-energy peaks and summing-in contributions to sum peaks, thereby affecting the measured full-energy peak efficiencies (FEPEs). The magnitude of the effect depends on the radionuclide decay scheme, detector characteristics, source-to-detector distance, and source geometry.

For a gamma-ray transition of energy E_i emitted in coincidence with one or more radiations of energies E_j, the TCS correction factor can be expressed as [18, 25]

$$C_{\text{TCS}}(E_i) = \frac{1}{1 - P_{\text{sum}}(E_i)}, \qquad (11)$$

where $P_{\text{sum}}(E_i)$is the total probability that the photon of energy $E_i$is detected in coincidence with one or more accompanying radiations emitted during the same decay cascade.

Neglecting angular-correlation effects, the summing probability may be written as

$$P_{\text{sum}}(E_i) = \sum_j I_j \bar{\epsilon}_t(E_j), \qquad (12)$$

where I_j is the emission probability of the coincident radiation E_j, and $\bar{\epsilon}_t(E_j)$ is the volume-averaged total efficiency corresponding to that radiation.

For the cylindrical source considered in the present work, the volume-averaged total efficiency is obtained by integrating the point total efficiency over the entire source volume according to

$$\bar{\epsilon}_t(E) = \frac{2}{S^2 H}\int_{h_0}^{h_0+H}\int_0^S F_{\text{self}}(E)\ \rho\, \epsilon_t(E, \rho, h)\, d\rho\, dh \qquad (13)$$

where S and H denote the radius and height of the cylindrical source, respectively, and $\epsilon_t(E, \rho, h)$ represents the total efficiency associated with a point located at radial coordinate ρ and axial coordinate h within the source volume, defined by Eq. (6).

Substituting Eq. (13) into Eq. (12) yields the coincidence summing correction factor for the cylindrical source geometry:

$$C_{\mathrm{TCS}}\left(E_i\right)=\left[1-\sum\ {}_jI_j\backslash\mathrm{hspace}\{0.17\mathrm{em}\}_{\epsilon\ t}^{-}\left(E_j\right)\right]^{-1}. \qquad (14)$$

The FEPE corrected for coincidence summing effects is then given by

$$\epsilon\ {}_{\mathrm{corr}}\left(E_i\right)=C_{\mathrm{TCS}}\left(E_i\right)\backslash\mathrm{hspace}\{0.17\mathrm{em}\}\epsilon\ {}_{\mathrm{cyl}}\left(E_i\right), \qquad (15)$$

where $\epsilon\ {}_{\mathrm{cyl}}\left(E_i\right)$ is the cylindrical-source FEPE calculated from Eq. (10).

For sufficiently large source-to-detector distances, the summing probability is generally small $\left(P_{\mathrm{sum}}\ll\ 1\right)$, and Eq. (14) may be approximated as

$$C_{\mathrm{TCS}}\left(E_i\right)\approx\ 1+\sum\ {}_jI_j\backslash\mathrm{hspace}\{0.17\mathrm{em}\}_{\epsilon\ t}^{-}\left(E_j\right). \qquad (16)$$

In the present work, the total efficiencies required for Eqs. (12)-(16) were calculated using the analytical detector-response formulation developed in Sections 2.1–2.3. The resulting coincidence-summing correction factors were subsequently applied to the calculated FEPE values and compared with the benchmark results reported by Demirel et al. [1].

In the present study, the investigated gamma-ray emissions originate from the radionuclides ^{210}Pb (46.5 keV), ^{234}Th (63.3 and 92.6 keV), ^{226}Ra (186.2 keV), ^{214}Pb (295.2 and 351.9 keV), $^{234\mathrm{m}}$Pa (1001.0 keV), and ^{214}Bi (609.3, 768.4, 1120.3, and 1764.5 keV). Among these radionuclides, ^{214}Pb and particularly ^{214}Bi are potential sources of true coincidence summing because several of their gamma-ray transitions are emitted in cascade during the same decay event. Consequently, the corresponding coincidence-summing probability may become non-negligible for close source-to-detector geometries and high-efficiency HPGe detectors. In contrast, the gamma-ray emissions of ^{210}Pb, ^{234}Th, ^{226}Ra, and $^{234\mathrm{m}}$Pa are either isolated or exhibit negligible coincidence effects; therefore, their contributions to TCS are expected to be insignificant.

The above formulation is fully compatible with the analytical efficiency model developed in the present work because it employs the same cylindrical-source geometry and volume-integration approach. Consequently, coincidence summing effects associated primarily with the cascade gamma-ray emissions of ^{214}Pb and ^{214}Bi can be incorporated directly into the calculated FEPE values without the need for Monte Carlo radiation-transport simulations. This approach provides a practical framework for assessing TCS corrections in cylindrical calibration and environmental samples measured with HPGe detectors.

2.5 Benchmark Source-Detector Geometry

The benchmark dataset analyzed in this study was obtained using a 78.5% relative-efficiency n-type coaxial HPGe detector. The active crystal dimensions were 62.8 mm in diameter and 73.8 mm in length, enclosed within an aluminum endcap of 69.9 mm diameter and 82.6 mm length. The detector entrance consisted of a 0.5-mm-thick beryllium window separated from the crystal by a 4-mm air gap as shown in Table 1.

Table 1
Detector specifications used in the DMM calculations [1].

Parameter	Value
Detector type	n-type coaxial HPGe
Relative efficiency	78.5%
Crystal diameter	62.8 mm
Crystal length	73.8 mm
Endcap diameter	69.9 mm
Endcap length	82.6 mm
Be window thickness	0.5 mm
Air gap	4.0 mm

Measurements were performed using cylindrical polypropylene containers having an inner diameter of 55 mm and a filling height of 35.5 mm. A 2-mm-thick polypropylene locator ensured reproducible coaxial positioning of the source relative to the detector as shown in Fig. 1. The source-detector configuration adopted in the DMM calculations is illustrated in Fig. 2.

The cylindrical source was modeled analytically as a homogeneous volume source characterized by radius S, height H, and source-to-detector distance h_0. Together with the detector radius $R$and crystal length L, these quantities define the geometrical framework of the Direct Mathematical Method used throughout this study.

4. Results and Discussion

The predictive performance of the Direct Mathematical Method (DMM) was evaluated by comparing the calculated full-energy peak efficiencies (FEPEs) with the experimental, RayXpert, and EFFTRAN results reported for the benchmark HPGe detector over the energy range 46.5-1764.5 keV. Relative deviations between the calculated and experimental efficiencies are summarized in Table 2. Notably, the DMM reduced the mean absolute relative deviation by approximately a factor of 14 compared with EFFTRAN and by a factor of 22 compared with RayXpert. This improvement demonstrates the effectiveness of the effective photopeak attenuation coefficient in representing detector response over a broad energy range.

Table 2
Comparison of full-energy peak efficiencies calculated using the Direct Mathematical Method (DMM), RayXpert, and EFFTRAN with the corresponding experimental values. Absolute relative deviations (|Relative Deviation|) are referenced to experimental efficiencies.

Energy (keV)	Experimental	DMM	RayXpert	EFFTRAN	|Relative Deviation| DMM (%)	|Relative Deviation| RayXpert (%)	|Relative Deviation| EFFTRAN (%)
46.539	0.130	0.13108	0.151	0.130	0.83	16.15	0.00
63.300	0.140	0.14036	0.161	0.144	0.26	15.00	2.86
92.590	0.128	0.12834	0.116	0.129	0.27	9.38	0.78
186.211	0.101	0.10109	0.114	0.100	0.09	12.87	0.99
295.224	0.073	0.07309	0.080	0.070	0.12	9.59	4.11
351.932	0.063	0.06307	0.069	0.060	0.11	9.52	4.76
609.312	0.041	0.04127	0.043	0.038	0.66	4.88	7.32
768.356	0.034	0.03413	0.036	0.032	0.38	5.88	5.88
1001.026	0.029	0.02893	0.030	0.026	0.25	3.45	10.34
1120.287	0.027	0.02725	0.028	0.024	0.92	3.70	11.11
1764.494	0.020	0.02006	0.020	0.018	0.32	0.00	10.00
Mean Absolute RD (%)					**0.38**	**8.22**	**5.29**

The DMM exhibited close agreement with the experimental data, with deviations ranging from 0.09% to 0.92% and a mean absolute relative deviation of only 0.38%. In comparison, the corresponding mean absolute deviations obtained using EFFTRAN and RayXpert were 5.29% and 8.22%, respectively. These results clearly demonstrate the superior predictive capability of the DMM across the entire investigated energy range.

Particularly good agreement was achieved at energies below 100 keV, where attenuation in the detector entrance window, dead layers, source container, and sample matrix strongly influences detector response. The small deviations observed in this region indicate that the analytical treatment of attenuation effects incorporated into the DMM provides an accurate representation of photon transport and interaction processes.

The comparison of true coincidence summing (TCS) correction factors is presented in Table 3. Overall, the DMM reproduced the benchmark TCS values with excellent accuracy, yielding relative deviations between 0.09% and 6.30% and a mean absolute relative deviation of 1.02%. The excellent agreement obtained for the ^{214}Bi cascade transitions is particularly important because these emissions are most susceptible to coincidence-summing effects and therefore constitute a stringent test of the proposed analytical model.

Table 3
Comparison of true coincidence summing correction factors calculated using the Direct Mathematical Method and those reported by Demirel et al. [1].

Radionuclide	Energy (MeV)	Present Study	Demirel, et al. [1]	Relative Deviation (%)
^{210}Pb	4.654E − 02	1.00829	1.0000	0.83
^{234}Th	6.330E − 02	1.00257	1.0700	6.30
^{234}Th	9.259E − 02	1.00267	1.0000	0.27
^{226}Ra	1.862E − 01	1.00090	1.0000	0.09
^{214}Pb	2.952E − 01	1.00124	1.0040	0.27
^{214}Pb	3.519E − 01	1.00106	0.9990	0.21
^{214}Bi	6.093E − 01	0.88006	0.8711	1.03
^{214}Bi	7.684E − 01*	0.88579	–	–
$^{234\varvec{m}}$Pa	1.001E + 00	0.99749	1.0060	0.85
^{214}Bi	1.120E + 00	0.85923	0.8575	0.20
^{214}Bi	1.764E + 00	1.00320	1.0050	0.18
Mean Absolute RD (%)				**1.02**

* The mean absolute relative deviation was calculated excluding the 768.4-keV ^{214}Bi transition, for which no benchmark value was reported by Demirel et al. [1].

For most gamma-ray emissions, the deviations remained below 1%, confirming the validity of the proposed analytical formulation for coincidence-summing calculations in cylindrical volume sources. The largest discrepancy was observed for the 63.3-keV transition of ^{234}Th, whereas the correction factors associated with the cascade-emitting radionuclide ^{214}Bi were reproduced with very good agreement. These findings demonstrate that the analytical framework can reliably account for coincidence-summing effects without requiring Monte Carlo radiation-transport simulations.

To further assess the predictive performance of the investigated methods, the coefficient of determination (R^2), root-mean-square error (RMSE), and mean absolute percentage error (MAPE) were calculated using the experimental efficiency values as reference data. As shown in Table 4, the DMM achieved the highest coefficient of determination ($R^2 = 0.99992$) together with the lowest RMSE (0.0015) and MAPE (0.38%). The statistical metrics consistently identify the DMM as the most accurate predictive model among the investigated approaches, yielding near-perfect agreement with the experimental efficiency dataset

Table 4
Statistical performance indicators of the investigated efficiency-calculation methods relative to the experimental full-energy peak efficiency data

Method	R²	RMSE	MAPE (%)
DMM	0.9999	0.0015	0.38
EFFTRAN	0.9978	0.0098	5.29
RayXpert	0.9946	0.0134	8.22
R² = coefficient of determination; RMSE = root-mean-square error; MAPE = mean absolute percentage error.			

5. Conclusions

The Direct Mathematical Method (DMM) was evaluated using the benchmark dataset reported by Demirel et al. for a 78.5% relative-efficiency n-type coaxial HPGe detector and compared with experimental measurements, EFFTRAN calculations, and Geant4-based RayXpert simulations over the energy range 46.5-1764.5 keV. The calculated FEPE values showed high level of agreement agreement with the experimental data, with absolute relative deviations ranging from 0.09% to 0.92% and a mean absolute relative deviation of only 0.38%. This performance significantly surpassed that of both EFFTRAN and Geant4-based RayXpert simulations, demonstrating the robustness of the analytical formulation over the entire investigated energy range. The statistical analysis further confirmed the accuracy of the DMM, yielding $R^2 = 0.99992$, RMSE = 0.0015, and MAPE = 0.38%. In

addition, the calculated true coincidence summing correction factors agreed closely with benchmark values, producing a mean absolute relative deviation of 1.02%.

Overall, the results demonstrate that the DMM provides an accurate and computationally efficient alternative to Monte Carlo simulation and efficiency-transfer techniques for HPGe detector efficiency calibration. Because the method requires only a limited set of detector and source parameters while eliminating the computational burden associated with particle-transport simulations, it represents a practical and reliable tool for detector characterization, efficiency calibration, coincidence-summing corrections, and routine gamma-ray spectrometry applications.

Declarations

Funding

The authors declare that no funds, grants, or other financial support were received during the preparation of this work.

Author Contribution

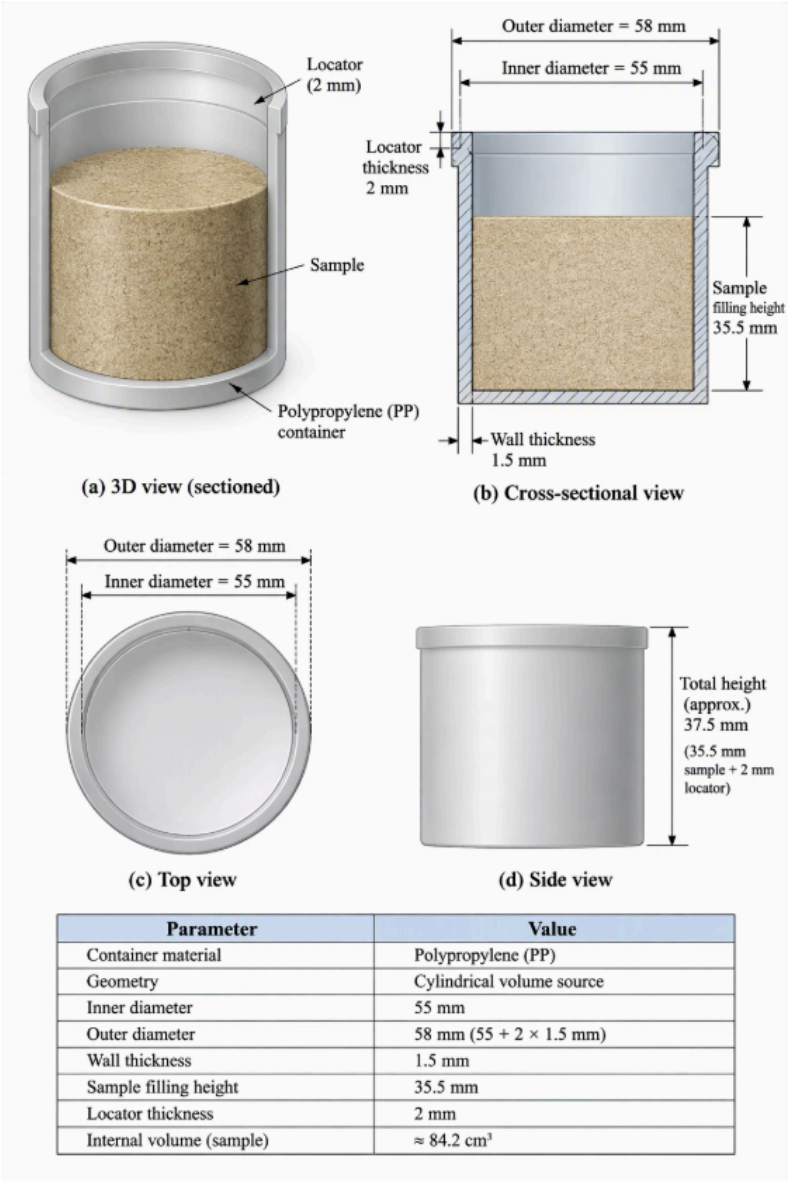
M.A.: Conceptualization; Methodology; Software; Validation; Formal analysis; Investigation; Data curation; Writing - original draft; Writing - review & editing; Visualization.

References

1. Demirel İ, Demirel SZ, Karanfil EC (2026) Development of a low-density calibration source prepared with polyurethane foam for HPGe detector gamma-ray spectrometry. Nucl Eng Technol 58:104843
2. Jodłowski P (2025) A simplified method for HPGe detector efficiency calibration using certified reference materials containing natural radionuclides. Appl Sci 15:9774
3. García-Durán A, Baltazar-Raigosa A, Ortega-Sígala JJ, Torres-Cortes CO (2026) FPGA-based simulator of HPGe gamma-ray spectra using RFID tokens as sources for educational and calibration applications. Nucl Eng Technol 58:104034
4. Parmentier A, Arcidiacono L, Senesi R, Romanelli G, Andreani C, Moir J, Festa G (2018) Absolute efficiency calibration of a coaxial HPGe detector for quantitative PGAA and T-PGAA. J Phys Conf Ser 1055:012010
5. Agostinelli S, Allison J, Amako K, Apostolakis J, Araujo H, Arce P, Asai M, Axen D, Banerjee S, Barrand G et al (2003) Geant4: a simulation toolkit. Nucl Instrum Methods Phys Res A 506:250–303
6. Vidmar T (2000) EFFTRAN: a Monte Carlo efficiency transfer code for gamma-ray spectrometry. Appl Radiat Isot 53:603–610
7. Vidmar T (2004) Applications of efficiency transfer calculations in gamma-ray spectrometry. Appl Radiat Isot 60:191–198
8. Allison J, Amako K, Apostolakis J et al (2016) Recent developments in Geant4. Nucl Instrum Methods Phys Res A 835:186–225
9. Sima O, Arnold D (2009) On the Monte Carlo simulation of HPGe gamma-spectrometry systems. Appl Radiat Isot 67:701–705
10. Jonsson S, Kastlander J, Vidmar T, Ramebäck H (2020) Experimental validation of correction factors for γ-γ and γ-X coincidence summing of ^133Ba, ^152Eu, and ^125Sb in volume sources. J Radioanal Nucl Chem 323:465–472
11. Ramebäck H, Jonsson S, Vidmar T (2021) Validation of EFFTRAN for efficiency transfer to distant geometries and volume sources. J Radioanal Nucl Chem 328:563–568
12. Verheyen L, Bruggeman M, Vidmar T, Boden S (2023) Validation of efficiency transfer for high-density materials in HPGe spectrometry. Appl Radiat Isot 194:110680
13. Abbas MI (2001) A direct mathematical method to calculate the efficiencies of a parallelepiped detector for an arbitrarily positioned point source. Radiat Phys Chem 60:3–9
14. Abbas MI (2006) Validation of analytical formulae for the efficiency calibration of gamma detectors used in laboratory and in situ measurements. Appl Radiat Isot 64:1661–1666
15. Abbas MI (2010) A direct mathematical method for HPGe efficiency calibration. Nucl Instrum Methods Phys Res A 621:413–418
16. Abbas MI (2024) A novel analytical method to calibrate cylindrical side-hole-type sodium iodide scintillation detectors. Appl Radiat Isot 205:111178
17. Abbas MI, Selim YS (2002) Calculation of relative full-energy peak efficiencies of well-type detectors. Nucl Instrum Methods Phys Res A 480:649–657
18. Abbas MI, Selim YS, Bassiouni MM (2001) HPGe detector photopeak efficiency calculation including self-absorption and coincidence corrections for cylindrical sources using compact analytical expressions. Radiat Phys Chem 61:429–431
19. Selim YS, Abbas MI (1994) Source-detector geometrical efficiency. Radiat Phys Chem 44:1–4
20. Sima O, Arnold D (2002) Transfer of the efficiency calibration of germanium gamma-ray detectors using the GESPECOR software. Appl Radiat Isot 56:71–75

21. Bosonnet S (1993) Calculation of the photopeak efficiency of germanium detectors. Nucl Instrum Methods Phys Res A 321:435–441
22. Wang TK, Mar WY, Ying TH, Tseng CL, Liao CH, Wang MY (1997) HPGe detector efficiency calibration for extended cylinder and Marinelli-beaker sources using the ESOLAN program. Appl Radiat Isot 48:83–95
23. Abbas MI (2001) HPGe detector photopeak efficiency calculation including self-absorption and coincidence corrections for Marinelli beaker sources using compact analytical expressions. Appl Radiat Isot 54:761–768
24. Hubbell JH, Seltzer SM (1995) Tables of X-Ray Mass Attenuation Coefficients and Mass Energy-Absorption Coefficients from 1 keV to 20 MeV for Elements Z = 1–92 and 48 Additional Substances of Dosimetric Interest. NISTIR 5632, National Institute of Standards and Technology, Gaithersburg, MD, USA
25. Gouda MM, Hamzawy A, Badawi1 MS, El-Khatib AM, Thabet AA, Abbas MI Mathematical method to calculate full-energy peak efficiency of detectors based on transfer technique. Indian J Phys (February 2016) 90(2):201–210. 10.1007/s12648-015-0737-1

Figures



Parameter	Value
Container material	Polypropylene (PP)
Geometry	Cylindrical volume source
Inner diameter	55 mm
Outer diameter	58 mm (55 + 2 × 1.5 mm)
Wall thickness	1.5 mm
Sample filling height	35.5 mm
Locator thickness	2 mm
Internal volume (sample)	≈ 84.2 cm^3

Figure 1

Geometry of the cylindrical polypropylene calibration container used in the benchmark measurements, showing the principal dimensions and sample configuration.

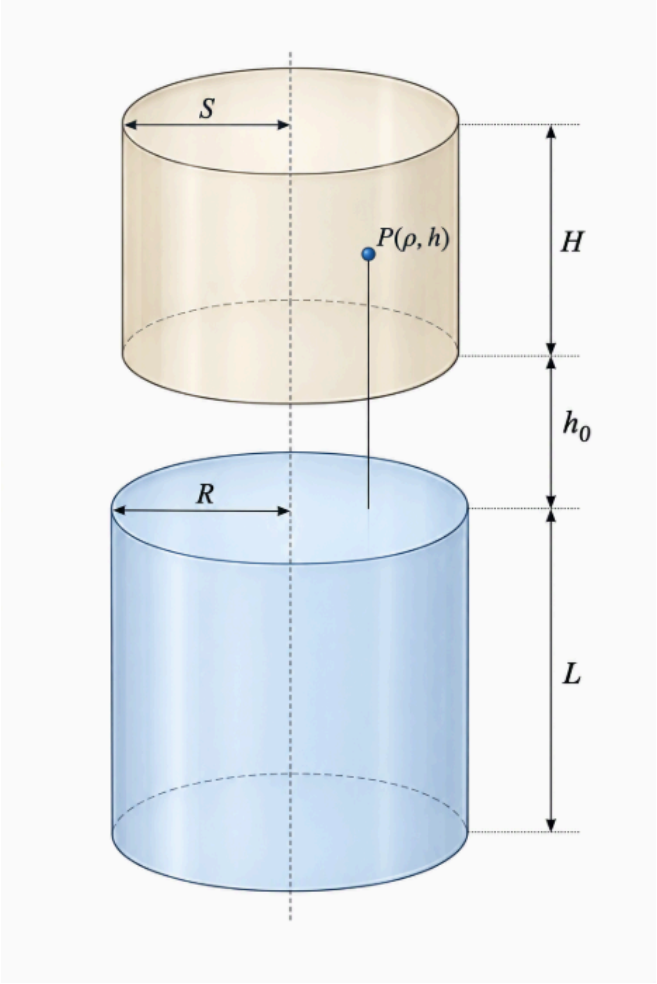


Figure 2

Analytical source-detector geometry employed in the Direct Mathematical Method (DMM) calculations. A cylindrical source of radius S and height H is positioned coaxially above a cylindrical HPGe detector of radius R and length L, separated by a source-to-detector distance h_0. The point P(ρ,h) denotes an arbitrary photon emission location within the source volume, defined in cylindrical coordinates.